Geomechanics and Engineering, *Vol. 37, No. 6 (2024) 555-563*
https://doi.org/10.12989/gae.2024.37.6.555

Study on damage law and width optimization design of coal pillar with the discrete element method

Chuanwei Zang[1], Bingzheng Jiang[1], Xiaoshan Wang*[2], Hao Wang[1], Jia Zhou[1], Miao Chen**[1] and Yu Cong[2]

[1]*College of Energy and Mining Engineering, Shandong University of Science and Technology, Qingdao, Shandong 266590, China*
[2]*School of Science, Qingdao University of Technology, Qingdao, Shandong 266590, China*

(*Received September 14, 2022, Revised May 10, 2024, Accepted May 14, 2024*)

Abstract. The reasonable setting of coal pillar width plays a key role in guaranteeing the steadiness of surrounding rock of fully mechanized caving gateroad driving along the next goaf. Based on the engineering background of the Bayangaole mine, the discrete element method was used to simulate the fracture evolution of coal pillars with different pillar widths. The results show that the damage rate of the coal pillar increases with the decrease in the width of the coal pillar. Once the coal pillar width is smaller than 6 m, cracks run through the coal pillar, and the coal pillar is completely damaged. In the middle of the coal pillar, which has a width of 6 m and above, there is a relatively complete area with low damage. The results show that the pillar width of 6 m is the most appropriate. Field tests prove that the reserved width of a 6 m small coal pillar can effectively control the surrounding rock deformation, ensuring the overall steadiness of the gateroad in the thick coal seam. It is hoped that this study will offer some reference for the determination of the reasonable size of the coal pillar.

Keywords: coal pillar; crack distribution; damage assessment; discrete element method; stress evolution

1. Introduction

The safe and efficient scientific mining and utilization of coal resources is of great importance for the sustainable development strategy of energy (Xie *et al.* 2012, Yang *et al.* 2021). During the coal mining process, a large number of gateroads are tunneling, about 4/5 of which are back mining gateroads. To protect the gateroad, coal pillars are usually left between the panels. The coal pillar is not only the basic bearing structure of the surrounding rock of the tunnel but also plays a vital role in isolating water and toxic gas and maintaining the stability of the gateroad. Therefore, this technology's core problem is to determine a reasonable coal pillar width to ensure the overall stability of the gateroad while improving the recovery rate (Salamon *et al.* 1967). Unreasonable coal pillar size will result in a state of yield for a long time, and the steadiness of the surrounding rock cannot be maintained (Jaiswal *et al.* 2009, Poulsen *et al.* 2014). Salamon (1970) applied the mechanism of laboratory compression test of brittle rock samples to mining and discussed the stability of the pillar. Hill *et al.* (2005) proposed a method for evaluating pillar stability through the safety factor method, which includes key geometric, geological, and statistical concepts related to pillar failure probability. Poulsen proposed a coal pillar load calculation method to evaluate the failure and stability of the coal pillar and compared it with the tributary zone theory to prove its rationality. Mahe *et al.* (2016) combined field experience and numerical tests to confirm the link between the width-height ratio of coal pillars and the squat effect, which offered a new design criterion. Zhang *et al.* (2017) studied the stress change and plastic zone distribution of coal pillars with different widths by combining numerical calculations and field tests, estimated the reasonable width of coal pillars, and proposed corresponding support strategies.

With the development of computer technology in recent years, numerical simulation has gradually become one of the leading research methods to study surrounding rock failure and reinforcement technology. Various numerical calculation methods have been developed and applied to mine stability analysis(Chen *et al.* 2022, 2023). Compared with the continuum model, Universal Distinct Element Code (UDEC) is a discrete element numerical simulation method that can be better applied to the failure process of coal and rock mass (Coulthard 1999, Lisjak *et al.* 2014). UDEC Trigon model is a discontinuous model supported by Voronoi logic, which can simulate the natural failure of rock mass more realistically than the traditional discrete element method (Lorig *et al.* 1989, Gao 2013). Gao *et al.* (2014) simulated the brittle failure of coal and granite and studied the shear failure process of gateroad roofs by using UDEC triangular block model. Zhang *et al.* (2017) used UDEC simulation to study coal slope failure mechanism and deformation during gob-side gateroad driving in deep mining. They put forward the control technology of high-strength pressure-length anchor cable combined with an anchor net.

As the mine enters deep mining, reasonable design of coal pillar width is the core issue to enhance the recovery

*Corresponding author, Associate Professor
E-mail: wangxiaoshan@qut.edu.cn
**Academic Professor
E-mail: miaochen@sdust.edu.cn

ISSN: 2005-307X (Print), 2092-6219 (Online)

rate of coal resources and ensure the recovery work's safety. If the coal pillar width is too large, it is difficult to improve the recovery factor, and if the coal pillar width is too small, the stability of the surrounding rock of the gateroad cannot be maintained. Taking the Bayangaole mine as an example, a wide coal pillar width of 30 m is adopted in the initial design. However, it was found in practical application that the 30 m coal pillar could cause waste of coal resources and cause stress concentration and rock burst. To effectively avoid mine disasters and improve the coal recovery rate, this paper applies the UDEC triangular block model to study the failure law of coal pillars with different sizes. Finally, a reasonable width setting for the coal pillar is put forward and validated by a field test.

2. Engineering background

The 311304 panel of Bayangaole Mine is located at the 311305 panel, which has an average burial depth of 610.7 m. The average thickness of the coal seam is 5.9 m, and the dip angle is 0°~1°. The geological histogram of the 311304 panels is shown in Fig. 1. The 311304 gateroad is driven along the gob-side of the 311305 gob, which has a height of 4.3 m and a width of 5.5 m. There is a 30 m-wide coal pillar between the gateroad and 311305 gob, as shown in Fig. 2.

Histogram	Lithology	Strata thickness /m	Buried depth /m
	Sandy mudstone	27	530.2
	Mudstone	18.3	548.5
	Sandy mudstone	6	554.5
	Medium sandstone	7.6	562.1
	Sandy mudstone	7.3	569.4
	Kern sandstone	17.3	586.7
	Sandy mudstone	8.1	594.8
	Medium sandstone	5.4	600.2
	Post sandstone	4.6	604.8
	Coal	5.9	610.7
	Mudstone	6.9	617.6
	Post sandstone	8.3	625.9

Fig. 1 Geological histogram of 311304 panel

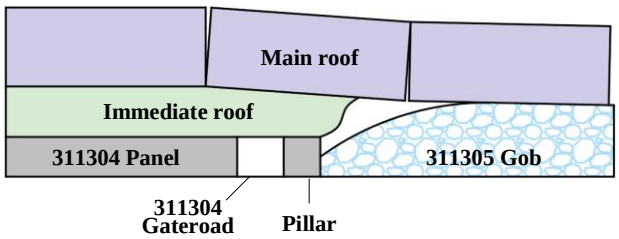

Fig. 2 Schematic diagram of gob-side pillar

3. Theoretical analysis

The overlying load distribution of the coal pillar is an important factor affecting its steadiness, and the stress state of the coal pillar, with distinguishing sizes, is different (He *et al*. 2019). When one side of the coal pillar is the gob, and the other side is the mining preparation gateroad, the stress peak value of the wide coal pillar on the side of the gob will be higher than that of the gateroad. The stress concentration area of the narrow coal pillar would also deviate to the side of the gob. When both sides of the coal pillar are gob, the overlying load on the coal pillar will be approximately symmetrically distributed. The overlying load distribution of the wide and narrow coal pillar is shown in Fig. 3. According to the analysis of the overlying rock structure and mechanics, the overlying load distribution of the wide coal pillar is bimodal, and the outer side of the goaf is the crushing zone I, and the stress gradually increases towards the inside, which is the plastic zone II, and then decreases after reaching the peak value. An elastic zone III is formed in the middle of the pillar, the minimum value of which is greater than or equal to γH (γ is the average bulk density of the overlying stratum, H is the height of the overlying stratum), that is the original rock stress; the overlying load distribution of the narrow coal pillar is unimodal, and from the outside to the inside are the crushing scope I, the plastic scope II and the elastic scope III

When the coal pillar width is larger, the elastic zone inside the coal pillar is large. The load is transferred to the coal pillar after the panel goes out, which will cause an outsized quantity of elastic energy to accumulate in the coal pillar. Mining and other activities may induce rock burst (Wu *et al.* 2023a, Wu *et al.* 2023b, Zhang *et al.* 2022). For example, the coal pillar left in the air return gateway of the 31102 panels of a mine in Inner Mongolia is 20 m. Strong mining pressure appears in the gateroad during the advance of the adjacent 31101 panels, accompanied by strong vibration and serious deformation, as shown in Fig. 4. After analysis and investigation, it is believed that the internal stress of the wide coal pillar is too concentrated, so the wide coal pillar cannot maintain the steadiness of the surrounding rock of the gateroad (Zhao *et al*. 2020).

A mass of practices has shown that the use of narrow coal pillars can increase coal production, and the vertical pressure of the overlying strata will be transferred to the solid coal side simultaneously, which is conducive to the stability of the gateroad. However, when the coal pillar width is too narrow, it will also be unstable due to insufficient bearing capacity. Therefore, a reasonable size not only requires sufficient elastic bearing area in the coal pillar but also avoids the waste of resources (He *et al*. 2020).

4. Discrete element numerical simulation

UDEC is a numerical simulation software of 2D supported by the discrete element method for discontinuous media, mainly used to analyze discontinuous media. Compared with other finite element software for analyzing

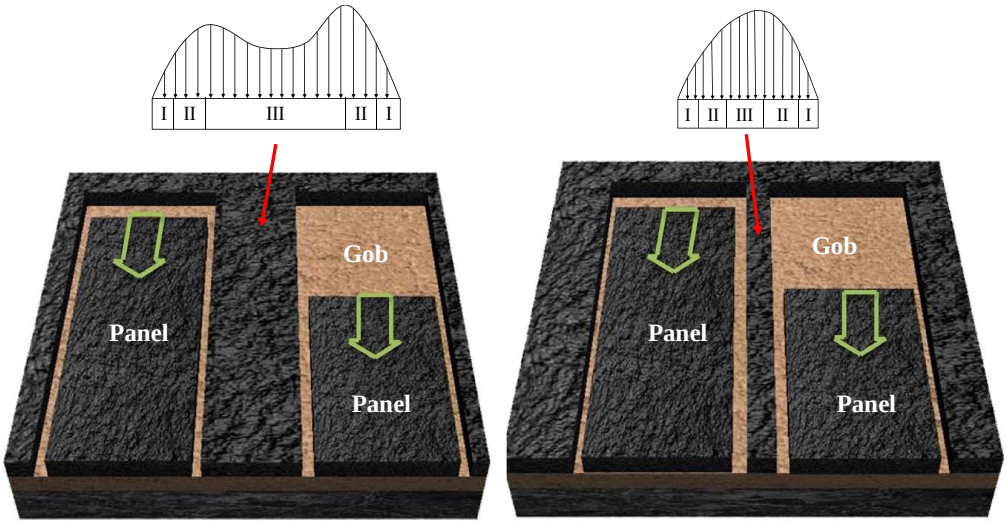

Wide pillar Narrow pillar

Fig. 3 Schematic diagram of overburden load of wide and narrow coal pillars

Fig. 4 Large deformation of gateroad caused by strong mining pressure

continuous media, the discrete element method (DEM) regards objects as a collection of discontinuous blocks and discontinuous contact surfaces between blocks. The macroscopic deformation and strength behavior of the numerical model rely on the mechanical parameters of the block and the contact surface. Because the rock material itself has the characteristics of joints and cracks, it has significant advantages to use the discrete element method of discontinuous medium to simulate and analyze the discontinuous fracture and overlying rock movement caused by underground mining. Therefore, UDEC is used to simulate and analyze the failure evolution law of coal pillars under different sections of coal pillar width.

In the simulation, the elastic constitutive model is adopted in the block; only deformation occurs when the block is subjected to external forces, but no damage occurs. As is shown in Fig. 5, the Mohr-Coulomb failure criterion is adopted in contact between blocks. In the normal and tangential direction of the contact surface, when the normal force or tangent force does not exceed the strength, the mechanical response behavior is dependent on the normal stiffness and tangent stiffness; when the normal force or tangential force exceeds the strength, tensile failure or shear failure occurs on the contact surface.

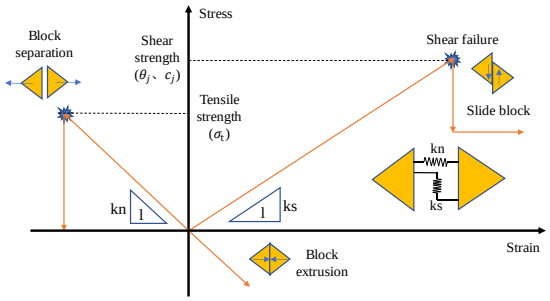

Fig. 5 Structural model of the block contact surface

Based on the geological conditions of the Bayangole 31104 panel, the numerical model of the surrounding rock was built to simulate the failure law of the coal pillar during mining. As shown in Fig. 6, the length of the model is 415 m and the height is 122.7 m. To enhance the calculation efficiency of the numerical model, small triangular blocks are only produced in the coal pillar and its surrounding area to study the damage and fracture distribution of the coal pillar, in which the maximum edge length of the triangular block in the coal seam area is 0.4 m. The maximum edge length of the triangular block in the range of roof and floor is 0.8 m, while rectangular blocks are used in other areas.

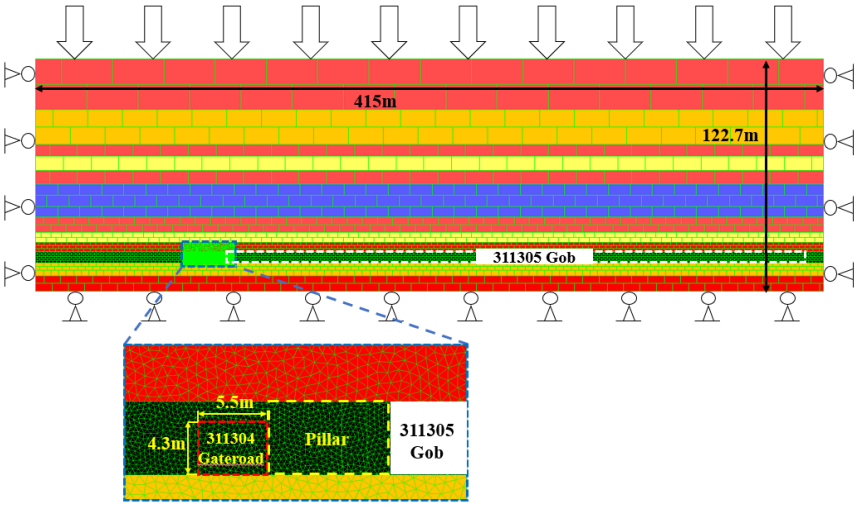

Fig. 6 UDEC numerical model

Table 1 Physical and mechanical property parameters of coal and rock mass

The lithology	Rock		RQD	Rock mass	
	E_r/ GPa	σ_c/ GPa		E_m/ GPa	σ_{cm}/ GPa
Sandy mudstone	18.36	21.8	81.98	7.56	12.47
Mudstone	13.50	22.6	75.32	4.18	10.80
Medium sandstone	32.92	25.2	90.43	19.47	18.10
Kern sandstone	26.90	23.9	82.19	11.18	13.75
Post sandstone	35.32	50.7	84.09	15.93	30.70
Coal	3.60	18.86	78	1.25	9.69

Displacement constraints are set on the model's left, right, and bottom boundaries, and 11.96 MPa loads are applied on the up boundary of the model to simulate the overburden load

The numerical model is first run to the equilibrium state to simulate the initial stress state, and then the gob and gateroad are simulated by deleting the block. Due to the influence of discontinuity of actual rock mass on mechanical parameters of rock mass, the mechanical parameters, just as compressive strength and Young's modulus measured by the indoor mechanical test, are quite different from those of actual rock mass. Based on the mechanical properties of the intact rock, the rock quality designation (RQD) value of the rock quality index of each rock layer is used as the measurement index (Zhang *et al.* 2004, Singh *et al.* 2005). The relationship between the modulus ratio E_m/E_r and RQD is established by formula (1), where E_r and E_m are the elastic modulus of the intact rock and rock mass, respectively. Elastic modulus of rock. The rock mass σcm compressive strength can be obtained by formula (2). According to the RQD data of coal and rock mass measured in the field, the estimated mechanical parameters are given in Table 1.

$$\frac{E_m}{E_r}=10^{0.0186RQD-1.91} \tag{1}$$

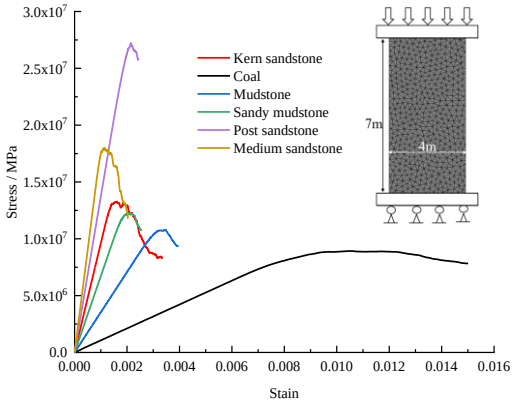

Fig. 7 Results of simulated uniaxial compression test

$$\frac{\sigma_{cm}}{\sigma_c}=\left(\frac{E_m}{E_r}\right)^q \tag{2}$$

The elastic and Mohr-Coulomb sliding models are used in block and contact surface models, respectively. A battery of simulated uniaxial compression tests are built, and the microscopic parameters of the UDEC model were calibrated using a trial-and-error method (Yang *et al.* 2017, Chen *et al.* 2016, Zang *et al.* 2020) to match the mechanical parameters of rock mass list in Table 1. The numerical simulation results are illustrated in Fig. 7, and the calibrated microscopic parameters used in the UDEC model are listed in Table 2.

5. Analysis of numerical simulation results

5.1 Analysis of damage evolution law of coal pillar

Affected by the mining of the previous panel and the excavation of the gateroad, the coal pillar will be disturbed by stress twice before and after the completion of the mining preparation gateroad, and the coal pillar will be damaged under the action of abutment pressure in this

Table 2 Microscopic parameters of the model after checking

The lithology	Block parameters			Joint parameters				
	Density/ (kg·m^{-3})	Bulk/GPa	Shear/Gpa	The normal stiffness /Gpa	Shear stiffness /Gpa	Cohesion /Mpa	Friction angle /°	Tensile strength /Mpa
Sandy mudstone	2610	4.35	3.13	458	185	2.61	34.3	1.14
Mudstone	2230	2.05	1.80	222.7	89.1	2.3	34.7	0.98
Medium sandstone	2290	14.75	7.61	1235	486	4.8	26	1.65
Kern sandstone	2360	5.82	4.74	607	243	3.5	26.3	1.37
Post sandstone	2320	8.43	6.72	869	348	4.7	42	3.07
Coal	1280	0.59	0.55	65.9	26.2	2.1	27	0.86

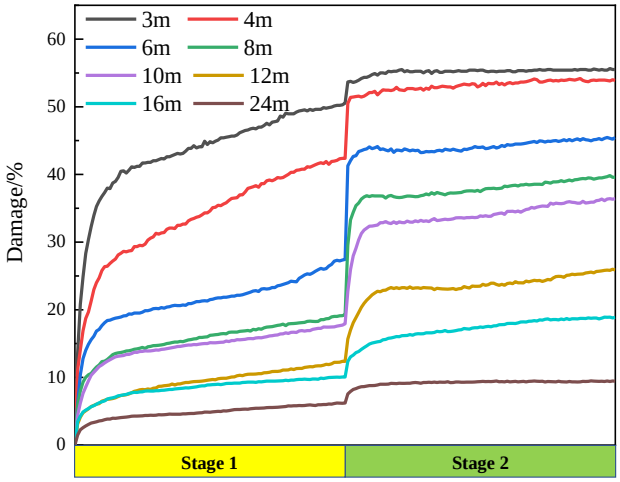

Fig. 8 Variation of coal pillar damage degree

process. To monitor the degree of damage to the coal pillar during excavation, the total number and length of cracks in the coal pillar are monitored by Fish language, and the damage parameter D is put forward.

$$D = \frac{N_S + N_T}{N_C} \times 100\% = \frac{N}{N_C} \times 100\% \quad (3)$$

Where N_S, N_t, N_c, and N are the length of the shear crack, tensile crack, joint and crack, respectively. The D is the damage parameter used to characterize the degree of damage to the coal pillar.

Fig. 8 shows the damage evolution process in coal pillars with different widths. The process can be seen in two stages: the excavation and stabilization process of the 311305 panel (stage 1) and the excavation and stabilization process of the 311304 panel (stage 2). In stage 1, it is evident that with the progress of mining, the damage degree of the coal pillar grows significantly at the initial stage of mining and then slows down gradually; at the final of stage 1, the damage degree of the coal pillar within the range of smaller pillar width (3 m~6 m) is larger, but the damage degree of the coal pillar decreases obviously with the increase of the remaining coal pillar width, which indicates that the damage of small coal pillar caused by the excavation disturbance of the previous panel is more serious. In stage 2, because of the disturbance of gateway excavation, the degree of damage to the coal pillar increased rapidly in the initial stage and then gradually stabilized. The damage degree of the 3 m coal pillar finally reached 55.6%, while the 24 m coal pillar is only 9.5%, which indicated that the larger the coal pillar width is, the smaller the damage degree of the coal pillar will be. It should be noted that due to the high degree of damage to the small size coal pillar (3 m) in the first stage, the excavation along the groove has little influence on it, and the growth rate of the damage to the coal pillar grows obviously with the increase of the coal pillar width. However, when the coal pillar size continued to increase to more than 16 m, the influence of the disturbance of the gateway excavation on the damage degree of the coal pillar began to weaken.

5.2 Analysis of damage degree of coal pillar

Influenced by the location of the gob and gateroad, the damage degree at different positions of coal pillar is not the same. To monitor the damage degree of coal pillars in different positions, the damage degree data for each meter of coal pillar is extracted by self-developed fish language. After the coal pillar is shaped, the damage degree at different positions of the coal pillar with different widths are shown in Fig. 9. As illustrated in Fig. 9, the area near the gateroad and gob is the most severely damaged area of the coal pillar, and the damage degree is distributed in a "U" shape. Gao (2013) proposed a critical value of 35% to divide the failure area, and this index is also used to assess the damage degree of the coal pillar in this analysis.

The simulated results show that the damage rate of each position of the coal pillar is more than 35% when the width of the coal pillar is 3 m and 4 m, indicating that the coal pillar at this size is in a state of severe damage, and the coal pillar is prone to deformation and instability. When the width is greater than 6 m, there is an area in the center of the coal pillar that is lower than the damage critical value, and the coal pillar in this area is relatively stable. And with the width of the coal pillar increasing continuously, this low-damage area is also gradually expanded. When the width increases from 16 to 24 m, there is an area with a damage degree of 0 in the center of the coal pillar, the complete elastic zone.

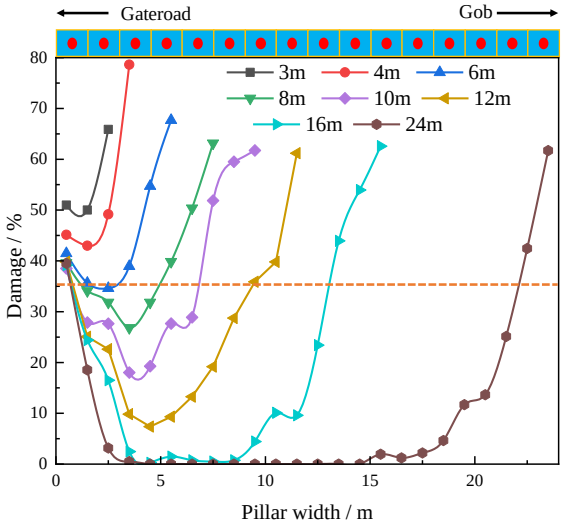

Fig. 9 Damage distribution of coal pillar

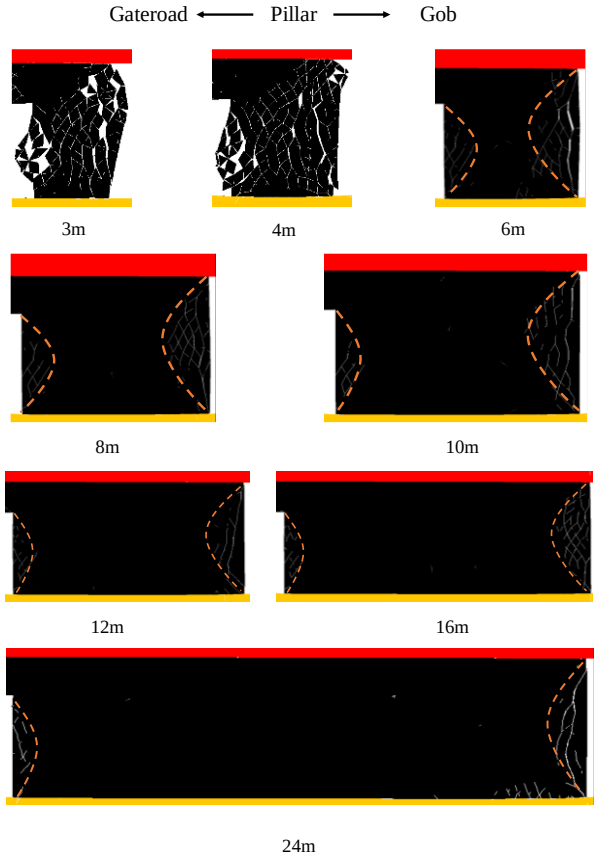

Fig. 10 Crack distribution of coal pillars with different widths

The fracture patterns and crack distributions of different coal pillar widths are shown in Fig. 10. It can be observed from the results that when the coal pillar width is 3 m and 4 m, the cracks on both sides of the coal pillar have run through, and the deformation of coal pillars are obvious.

When the width of the coal pillar comes to 6 m, the crack concentration area caused by excavation is mainly concentrated on both sides of the coal pillar, and there is a relatively complete low damage area in the middle of the coal pillar. The width of the crack density area on the side of the gateroad is about 1-2 m, and that on the side of the gob is about 2-3 m. With the increase of coal pillar width, the width of the crack dense area on the side of the gateroad and gob is close to 6 m when the width is 8 m, and the proportion of low damage area in the center of the coal pillar has increased. When the width rises to more than 10 m, the width of the crack dense area on the side of the gateroad is about 1m, and that on the side of the gob is about 2-3 m. That is, when the width is more than 6 m, the macroscopic failure range of the coal pillar does not increase significantly. With the increase of the coal pillar width, the proportion of low damage area in the center of the coal pillar increases gradually, consistent with the distribution characteristics of the high damage area. Therefore, it is noted that when choosing a reasonable coal pillar width, attention should be paid to the change of the high-damage area. When the coal pillar width is decreased, the high damage areas on both sides will gradually approach and expand until macroscopic through-fractures are formed. Therefore, it is indispensable to avoid the collapse of coal pillars because they are too close to connect the fractures

5.3 Analysis of the overlying load of coal pillar

To study the change in the overlying load of the coal pillar, a monitoring line is arranged above the coal pillar, and the overlying load under the coal pillar with different widths is recorded. As shown in Fig. 11, the overlying load shows a bimodal distribution when the coal pillar width is 24 m and the peak area is close to the gob. With the decrease of the width of the coal pillar, the peak area gradually shifts to the gateroad. When the coal pillar width is between 10 m and 16 m, the peak value of the overlying load of the coal pillar increases with the decrease of coal pillar width, while the peak value of the overlying load of the coal pillar begins to reduce with the reduction of the coal pillar width (8 m to 6 m). The peak value of the overlying load decreases sharply when the width is from 4 m to 3 m. At the same time, the pressure on the left side of

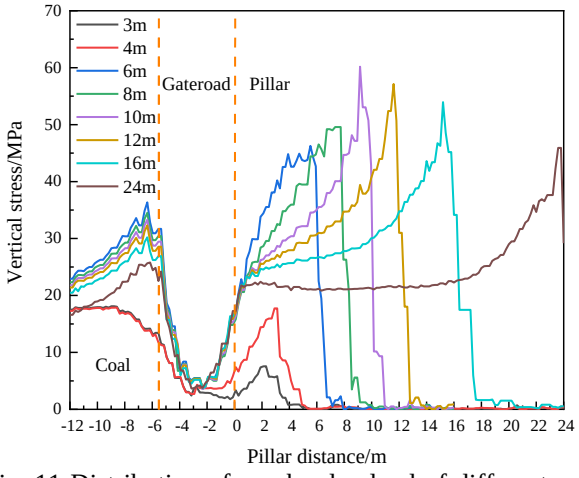

Fig. 11 Distribution of overburden load of different coal pillars

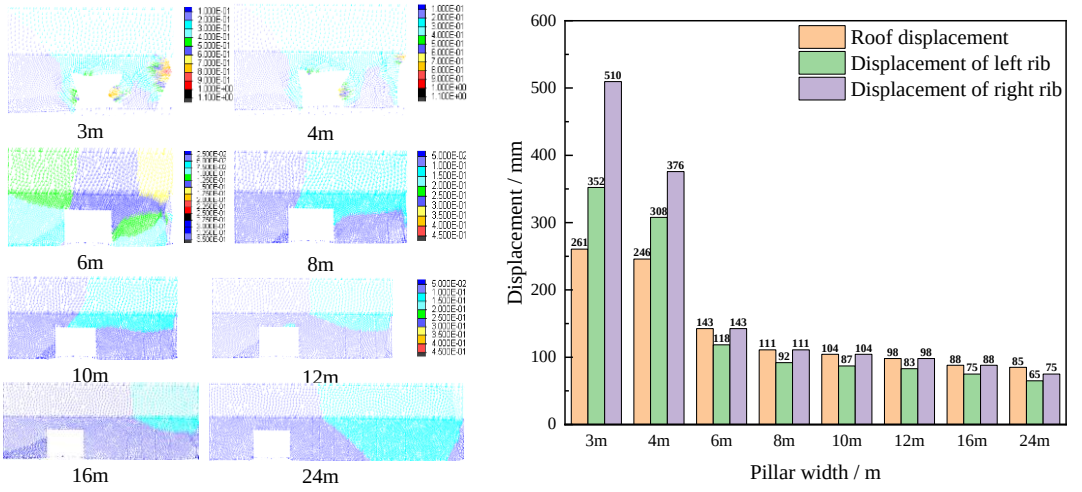

(a) Displacement vector diagram (b) Displacement variation of gateroad surrounding rock

Fig. 12 Displacement comparison diagram of gateroad with different coal pillars widths

the gateroad increases gradually when the width is from 24 m to 6 m, with a decrease in the width of the coal pillar and sharply when the width is 4 m and 3 m. The former is that the load gradually shifted to the left side of the gateroad, while the latter is the pressure relief phenomenon caused by the coal side failure.

Compared with Fig. 7, it can be seen that this is a pressure relief phenomenon caused by the decrease of the pressure-bearing capacity of the coal pillar when the overall damage degree increases. From the above investigation, it is known that we need to pay attention to the change of bearing pressure of the coal pillar when selecting the coal pillar width. When the damage of the coal pillar reaches a certain level, the pressure relief phenomenon that the peak value of the overlying load decreases, which is often the beginning of the coal pillar becoming unstable and leading to the collapse, and the peak value of the overlying load will be greatly reduced when the coal pillar collapses. Therefore, it is indispensable to leave a coal pillar of sufficient width to prevent the expansion of its damage.

5.4 Gateroad deformation analysis

Figs. 12(a) and 12(b) shows the displacement vector diagram and variation of gateroad with different widths of coal pillars. The numerical results show that the displacement of the gateroad roof and both sides continues to increase with the decrease of the coal pillar width, and the displacement of the right side is always more significant than the left side, as shown in Fig. 12(a). As the coal pillar widths exceed 6 m, the displacement grows slowly with the increasing widths. When the width of the coal pillar is 6 m, the displacement of the roof, left and right sides of the gateroad reached 143 mm, 118 mm, and 143 mm, respectively, and the gateroad is relatively stable; while when the width of the coal pillar is less than 6 m, the displacements of the surrounding rock increase significantly. Therefore, the width of the reserved coal pillar should be 6 m or above to maintain the stability of the gateroad.

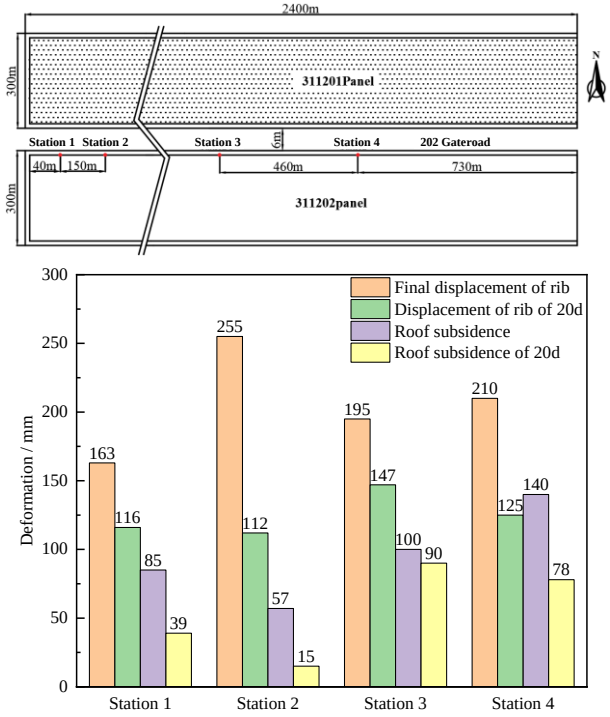

Fig. 13 Station layout and gateroad deformation data

5.5 Field test

To verify whether the coal pillar (6 m) can meet the stability requirements of the surrounding rock, a 311201 panel with similar geological conditions is selected for the engineering test. As illustrated in Fig. 13, monitoring stations are arranged along the return air trough in the 311302 panels, and the gateroad deformation in the case of a 6m narrow coal pillar is shown in Fig. 13.

The results of monitoring show that the deformation of rocks surrounding the gateroad is controlled effectively, and the maximum deformation of the gateroad roof and two sides within 20 days of excavation is 90 mm and 147 mm, respectively. After the surrounding rock deformation is

stabilized, the maximum subsidence of the roof and the deformation of both sides reach 140 mm and 255 mm, respectively. The field test result shows that the surrounding rock's deformation is within an acceptable range, and there are no dynamic phenomena such as rockburst, which proves the rationality of the setting of a 6 m narrow coal pillar.

6. Conclusions

In order to determine the reasonable coal pillar size to ensure the stability of the surrounding rock of the gob roadway, the fracture evolution distribution law of the coal pillar under different coal pillar widths is simulated by a discrete element numerical simulation method based on the mining geological conditions of the Bayangole 311305 panel. The following conclusions can be obtained:

(1) With the decrease of the coal pillar width, the overall damage rate of the coal pillar is continuously increasing, and the damage is concentrated on the side of the gob and gateroad. The high damage area on both sides of the coal pillar is close to the middle of the coal pillar, and the coal pillar is completely destroyed when the coal pillar width is below 6 m, while there is a relatively complete low damage area in the middle of the coal pillar for the coal pillar width greater than 6 m.

(2) The pressure relief phenomenon is caused by the decrease of the pressure-bearing capacity of the coal pillar when the overall damage rate increases. The overlying load concentration area of the coal pillar approaches the side of the gateroad with the decrease of the coal pillar width and reaches the peak at 10 m. The pressure-bearing capacity of the coal pillar decreases significantly at 4 m. The overburden load on the left side of the gateroad increases continuously with the decrease of the coal pillar width and decreases sharply at 4 m.

(3) The displacement cloud map results under different coal pillar widths show that the surrounding rock deforms seriously when the coal pillar size is less than 6 m, and the deformation is small and relatively stable when the coal pillar size is more than 6 m. The field-measured data also show that the surrounding rock deformation can meet the design requirements when using a 6 m narrow coal pillar, which ensures the stability of the mining preparation gateroad.

Declaration of competing interest

The authors declare that they have no known competing financial interests or personal relationships that could have appeared to influence the work reported in this paper.

Acknowledgements

The research was supported by the National Natural Science Foundation of China (52374128, 42207201, 52004145) and the Natural Science Foundation of Shandong Province(ZR2020QE119).

References

Chen, M., Yang, S.Q., Zhang, Y.C. and Zang, C.W. (2016), "Analysis of the failure mechanism and support technology for the Dongtan deep coal roadway", *Geomech. Eng.*, **11**(3), 401-420. https://doi.org/10.12989/gae.2016.11.3.401.

Chen, M., Zang, C.W., Ding, Z.W., Zhou, G.L., Jiang, B.Y., Zhang, G.C. and Zhang, C.P. (2022), "Effects of confining pressure on deformation failure behavior of jointed rock", *J. Central South Univ.*, **29**(4), 1305-1319. https://doi.org/10.1007/s11771-022-4991-z.

Chen, M., Zhang, Y.L., Zhang, G.C., Zhou, G.L. and Wang, Z.H. (2023), "Discrete element study on mechanical response and pressure relief effect of rock containing variable hole", *Theor. Appl. Fract. Mech.*, **127**, 103976. https://doi.org/10.1016/j.tafmec.2023.103976.

Coulthard, M.A. (1999), "Applications of numerical modelling in underground mining and construction", *Geotech. Geol. Eng.*, **17**, 373-385. https://doi.org/10.1023/A:1008951216602.

Gao, F.Q. (2013), "Simulation of failure mechanisms around under-ground coal mine openings using discrete element modelling", PhD thesis. Simon Fraster University, Burnaby.

Gao, F.Q. and Stead, D. (2014), "The applicationofa modified Voronoi logicto brittle fracture modelling at the laboratory and fieldscale", *Int. J. Rock Mech. Min. Sci.*, **68**, 1-14. https://doi.org/10.1016/j.ijrmms.2014.02.003.

He, W., He, F. and Zhao, Y. (2019), "Field and simulation study of the rational coal pillar width in extra-thick coal seams", *Energ. Sci. Eng.*, **8**(1).

He, W.R., He, F.L., Chen, D.D. and Chen, Q.K. (2020), "Coal pillar width and surrounding rock control of roadway driving along goaf in fully mechanized top coal caving face", *J. Min. Saf. Eng.*, **37**(2), 349.

Hill, D. (2005), "Coal pillar design criteria for surface protection", *Proceedings of the coal conference*.

Jaiswal, A. and Shrivastva, B.K. (2009), "Numerical simulation of coal pillar strength", *Int. J. Rock Mech. Min. Sci.*, **46**(4), 779-788. https://doi.org/10.1016/j.ijrmms.2008.11.003.

Lisjak, A. and Grasselli, G. (2014), "A review of discrete modeling techniques for fracturing processes in discontinuous rock masses", *J. Rock Mech. Geotech. Eng.*, **6**(4), 301-314. https://doi.org/10.1016/j.jrmge.2013.12.007.

Lorig, L.J. and Cundall, P.A. (1989), "Modeling of reinforced concrete using the distinct element method", *Springer New York*.

Mathey, M. and Merwe, J.N.V.D. (2016), "Critique of the South African squat coal pillar strength formula", *J. South Afr. Inst. Min. Metall.*, **116**(3), 291-299. https://doi.org/10.17159/2411-9717/2016/v116n3a11.

Poulsen, B.A., Shen, B., Williams, D.J., Huddlestone-Holmes, C., Erarslan, N. and Qin, J. (2014), "Strength reduction on saturation of coal and coal measures rocks with implications for coal pillar strength", *Int. J. Rock Mech. Min. Sci.*, **71**, 41-52. https://doi.org/10.1016/j.ijrmms.2014.06.012.

Salamon, M.D.G. (1970), "Stability instability and design of pillar workings", *Int. J. Rock Mech. Min. Sci. Geomech.*, **7**(6), 613-631. https://doi.org/10.1016/0148-9062(70)90022-7.

Salamon, M.D.G. and Munro, A.H. (1967), "A Study of the strength of coal pillars", *J. South. Afr. Inst. Min. Metall.*, **68**(2), 55-67. https://hdl.handle.net/10520/AJA0038223X_3918.

Singh, M. and Seshagiri, R.K. (2005), "Empirical methods to estimate the strength of jointed rock masses", *Eng. Geol.*, 77(1-2), 127-137. https://doi.org/10.1016/j.enggeo.2004.09.001.

Wu, S.K., Zhang, J.W., Song, Z.X., Fan, W.B., Zhang, Y., Dong, X.K. and Ma, S.J. (2023a), "Review of the development status of rock burst disaster prevention system in China", *J. Central South Univ.*, **30**(11), 3763-3789. https://doi.org/10.1007/s11771-

023-5478-2.

Wu, W.X. and Gong, F.Q. (2023b), "Dynamic tensile strength weakening effect of pretension stressed red sandstone under impact load", *J. Central South Univ*., **30**(10), 3349-3360. https://doi.org/10.1007/s11771-023-5420-7.

Xie, H.P., Zhou, H.W., Xue, D.J., Wang, H.W., Zhang, R. and Gao, F. (2012), "Research and thinking on deep mining and limit mining depth of coal", *J. China Coal Soc.*, **37**(4), 535-542.

Yang, H.R., Ning, S.Z., Ding, L. and Liu, Z. (2021), "Research on the current situation and countermeasures of my country's coal industry in the new era", *China Coal Geol*., **33**(1), 44.

Yang, S.Q., Chen, M., Jing, H.W., Chen, K.F. and Meng, B. (2017), "A case study on large deformation failure mechanism of deep soft rock roadway in Xin'An coal mine, China", *Eng. Geol.*, **217**, 89-101. https://doi.org/10.1016/j.enggeo.2016.12.012.

Zang, C.W., Chen, M., Zhang, G.C., Wang, K. and Gu, D.D. (2020), "Research on the failure process and stability control technology in a deep roadway: Numerical simulation and field test", *Energ. Sci. Eng.*, **8**, 1-14. https://doi.org/10.1002/ese3.664.

Zang, C.W., Zhou, J., Chen, M., Bai, F. and Zhao, Z.Y. (2023), "Study on the instability mechanism of coal and rock mining under a residual coal pillar in gently inclined short-distance coal seam with the discrete element", *Sustainability*, **15**(7), 6294. https://doi.org/10.3390/su15076294.

Zhang, G.C., He, F.L., Jia, H.G. and Lai, Y.H. (2017), "Analysis of gateroad stability in relation to yield pillar size: A case study", *Rock Mech. Rock Eng.*, **50**(5), 1263-1278. https://doi.org/10.1007/s00603-016-1155-1.

Zhang, G.C., Li, Y., Meng, X.J., Tao, G.Z., Wang, L., Gao, H., Zhu, C., Zou, H. and Qu, Z. (2022), "Distribution law of in situ stress and its engineering application in rock burst control in Juye mining area", *Energies*, **15**(4), 1267. https://doi.org/10.3390/en15041267.

Zhang, L. and Einstein, H.H. (2004), "Using RQD to estimate the deformation modulus of rock masses", *Int. J. Rock Mech. Min. Sci.*, **41**(2), 337-341. https://doi.org/10.1016/S1365-1609(03)00100-X.

Zhang, Y.C., Yang, S.Q., Chen, M and Zang, C.W. (2017), "Deformation and failure mechanism and control technology of solid coal slope of roadway driving along goaf in fully mechanized top coal caving in deep mine", *Rock Soil Mech.*, **38**(4), 1103.

Zhao, Y.X., Zhou, J.L. and Liu, W.G. (2020), "Analysis of loading characteristics and impact instability law of deep mining adjacent goaf roadway in Xinjie mining area", *J. China Coal Soc.*, 0545(5), 1595-1606.